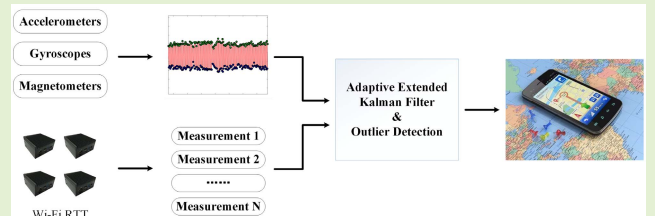


Kalman Filter-Based Data Fusion of Wi-Fi RTT and PDR for Indoor Localization

Xu Liu, Baoding Zhou^{ID}, Panpan Huang, Weixing Xue^{ID}, Qingquan Li^{ID},
Jiasong Zhu, and Li Qiu^{ID}, Member, IEEE

Abstract—The Fine Time Measurement (FTM) protocol introduced by IEEE 802.11 includes a new ranging method, named Wi-Fi Round Trip Time (Wi-Fi RTT), which can be used for indoor localization. Pedestrian Dead Reckoning (PDR) can provide accurate pedestrian tracking through inertial sensors in a short time. Information fusion of PDR and existing wireless technology is widely used in indoor localization to ensure the robustness and stability. In this paper, we propose a fusion indoor localization method of Wi-Fi RTT and PDR. Firstly, an adaptive filtering system consisting of multiple Extended Kalman Filter (EKF) and a new outlier detection method is proposed to reduce the localization error of Wi-Fi RTT. Secondly, the fusion algorithm based on the Federated Filter (FF) and observability is designed to combine Wi-Fi RTT with PDR. Finally, to further improve the localization performance of the fusion algorithm, a real-time smoothing method with fixed interval is used. We evaluate the proposed method in four different scenarios. The results show that the proposed indoor localization method has better stability and robustness, and the average localization error decreased by 37.4–67.6% compared with the classic EKF-based method.

Index Terms—Wi-Fi round trip time (RTT)/Wi-Fi fine time measurements (FTMs), pedestrian dead reckoning (PDR), indoor localization, fixed-interval filter, extended Kalman filter.



I. INTRODUCTION

INDOOR localization is a key technique in Localization-Based Services (LBS), since people spend the majority of their time indoors [1]–[3]. Currently, a smartphone is usually equipped with various sensors, including inertial measurement units, Wi-Fi, camera *et al.*, which makes it a useful device for indoor localization.

Wi-Fi localization is widely used for smartphone-based indoor localization [5], [6]. There are two mainly categories of Wi-Fi localization methods: Wi-Fi fingerprinting [5], [7], [8] and ranging measurement-based method [9]–[11]. Wi-Fi fingerprinting method needs to collect and update fingerprints, which is time-consuming and labor-intensive [12]. Moreover, due to the uncertainty of the environment, the fluctuation of wireless signal leads to the great change of RSSIs, which

Manuscript received December 16, 2020; accepted January 5, 2021. Date of publication January 11, 2021; date of current version February 17, 2021. This work was supported in part by the National Nature Science Foundation of China under Grant 41701519, in part by the Guangdong Basic and Applied Basic Research Foundation under Grant 2019A1515011910 and Grant 2019A1515111212, in part by the Shenzhen Scientific Research and Development Funding Program under Grant JCYJ20190808113603556 and Grant KQTD20180412181337494, and in part by the China Postdoctoral Science Foundation under Grant 2019M663069. The associate editor coordinating the review of this article and approving it for publication was Prof. Dongsoo Han. (Corresponding author: Baoding Zhou.)

Please see the Acknowledgment section of this article for the author affiliations.

Digital Object Identifier 10.1109/JSEN.2021.3050456

poses a challenge to stable localization accuracy. Ranging measurement-based localization methods can be divided into two types: time-based methods and Received Signal Strength-based (RSS-based) methods [9], [13]. Time-based Wi-Fi localization requires high-precision time synchronization. However, the general commercial Wi-Fi Access Points (APs) cannot realize high-precision time synchronization. RSS-based Wi-Fi localization systems require accurate propagation models. The RSS measurements are severely affected by the indoor environment [14]. Therefore, it is difficult to establish an accurate propagation model, resulting in poor accuracy.

In 2013, to achieve high-accuracy indoor localization with a simple localization calculation procedure, a new Wi-Fi protocol, called Wi-Fi Time of Flight (Wi-Fi ToF) is proposed [15]. By measuring round-trip delays, Wi-Fi RTT can compensate for the asynchronous between the transmitter and the receiver and achieve accurate localization information. Recently, IEEE 802.11-2016 proposed a Fine Time Measurement (FTM) protocol, also called Wi-Fi RTT, which can offer meter-level accuracy [16]. Intel's research team has standardized the protocol and allowed users to establish connections to a base station via a mobile device and obtain information for localization, such as the MAC address, time, distance from the device to the base station, RSSI, and number of successful measurements. Compared with the traditional ranging measurement-based method, Wi-Fi

RTT ranging system has relatively high accuracy and does not require manual synchronization between the base station and the mobile device, which reduces the system complexity. However, in complex indoor environments, Wi-Fi RTT suffers from challenges, such as multipath interference and packet loss, which affect its localization performance. When packet loss occurs simultaneously among all devices, the Wi-Fi RTT localization system cannot work normally.

As a common indoor localization method, Pedestrian Dead Reckoning (PDR) [17] can effectively improve the performance of radio frequency signal-based localization systems. In PDR, inertial data obtained by the accelerometer and gyroscope are used to calculate step detection, step length estimation and heading estimation. Then, combined with the known starting point, the position is obtained through continuous iterative calculation. The advantage of PDR is that it does not require the assistance of external sensors and can realize relative localization in a short time. Nevertheless, PDR also faces some shortcomings [18]: 1) The cumulative error of PDR will increase continually with time. 2) PDR can only realize relative localization, which requires a known starting position.

The fusion localization system based on PDR and wireless technology can provide better robustness [19]. There are many complementarities between Wi-Fi RTT and PDR. The PDR localization error can be adjusted or reset by Wi-Fi RTT. At the same time, PDR can provide more accurate localization results in a short time, thereby overcoming the Wi-Fi RTT packet loss and keeping the localization system stable.

To enhance the localization performance in terms of localization accuracy and stability, a new indoor localization method that fuses the Wi-Fi RTT ranging technology with PDR is proposed. The main contributions of the proposed algorithm are listed as follows:

- 1) An adaptive filtering system named position-tracking adaptive EKF composed of a set of EKF is proposed, which will be used to obtain RTT localization results and select the optimal filtering parameters. Moreover, an outlier detection method based on the optimal state estimation and residual detection is proposed to reduce the packet loss rate and measurement jump rate of Wi-Fi RTT. This method can efficiently detect the outliers in each set of measurements under the condition of severe packet loss.
- 2) A fusion-tracking Federated Filter (FF)-based indoor localization method is proposed to fuse Wi-Fi RTT and PDR. Different from existing localization methods based on Wi-Fi RTT, this method fuses Wi-Fi RTT and PDR using a federated filter based on observability. Then, the method corrects the position error caused by sensor drift in the pure PDR system using the fusion localization results.
- 3) To improve the robustness of the localization system, a fixed-interval smoothing method is proposed. This method first utilizes a backward filter to process the fusion-tracking EKF-based results. Then, it uses a weight-based fusion algorithm to fuse the backward filter results and fusion tracking results.

The remainder of this paper is organized as follows. Section II reviews the related works. Section III describes the fusion method of Wi-Fi RTT and PDR based on Federated Filter (FF) in detail. Section IV provides the experimental results and corresponding discussion. Finally, the conclusion is present in Section V.

II. RELATED WORKS

Wi-Fi RTT localization has become a research hotspot due to it can achieve meter-level indoor localization [16]. Many indoor localization methods based on Wi-Fi RTT have been proposed [20]–[22]. A three-step-localization method is proposed in [20] to overcome the problem of no or multiple intersect points in Wi-Fi RTT trilateration. It is observed in [20] that the method consists of systematic bias determination and removal, Clustering-based Trilateration (CbT) supported by Weighted Concentric Circle Generation (WCCG), and a Kalman filter. This method achieves a dynamic localization accuracy of 1.3m, but the effect of interference from obstacles is unknown. Guo *et al.* [21] proposed an integrated ranging algorithm based on Wi-Fi RTT and received signal strength (RSS) to enhance the scalability and robustness of the localization system. However, this method requires a correction algorithm to compensate the Wi-Fi RTT measurements, resulting in a mismatch between the Wi-Fi RTT measurements and the corresponding standard deviation. Yan *et al.* [22] proposed a multi-dimensional scaling-based localization algorithm to reduce the indoor multipath effects. In the case of severe fluctuation in the Wi-Fi RTT ranging results, the weighted mechanism used in [22] may cause large localization errors.

PDR is a common indoor localization method for smartphone [17]. A PDR system mainly includes three main tasks: step detection, step length estimation and heading estimation. One of the most challenge of PDR is the accumulative error caused by the step length and heading estimation. Some approaches have been proposed to solve this issue [23], [24]. Poulose *et al.* [23] present a comparative analysis of different sensor fusion techniques for heading estimation to find the best heading estimation method suitable for PDR. In addition, Tao *et al.* [24] uses time-differenced carrier phase (TDCP) technique to improve the performance of PDR system. This method can estimate displacement by processing differences of consecutive carrier phase measurements obtained from GNSS. Moreover, Huang *et al.* [25] proposed an algorithm which integrate strap-down inertial navigation and PDR to improve the accuracy of pedestrian tracking through reducing the cumulative error. However, smartphone-based PDR is unable to achieve long-time localization due to the accumulate error.

In recent years, some methods have been proposed to utilize PDR to improve the accuracy of Wi-Fi [26]–[28]. A robust dead-reckoning algorithm based on Wi-Fi RTT and multi-sensor was proposed in [26]. This method can reduce the Wi-Fi RTT ranging errors and achieve accurate localization in the complex indoor environment compared to the traditional dead reckoning method. However, this method needs to be improved in terms of long-term localization performance. Sun *et al.* [27] proposed an Adaptive Wi-Fi FTM localization

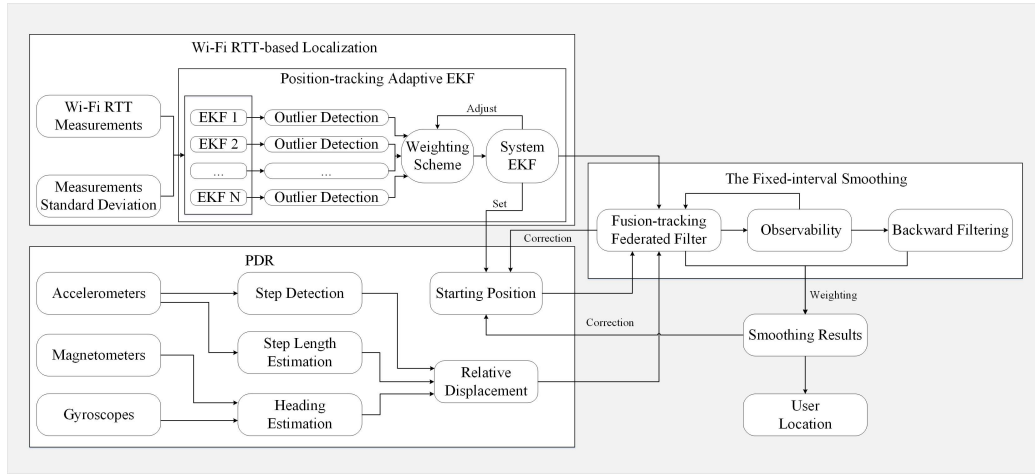


Fig. 1. Proposed indoor localization system.

algorithm (AWFP) method to compensate the Wi-Fi RTT measurements. The weight factor of AWFP method is adjusted by calculating the confidence based on the compensation error. However, the AWFP method may be unstable when the Wi-Fi RTT measurements change drastically caused by multipath. In addition, an enhanced particle filter-based (PF-based) fusion method with a new criterion for divergence monitoring and rapid re-initialization is proposed to integrate the advantages of PDR and Wi-Fi RTT [28]. Experimental results show that the proposed fusion method has better localization performance than the single-source localization method in complex indoor environment. However, this PF-based fusion method has the problem of large amount of calculation and poor stability.

To overcome the shortcomings of the existing fusion algorithms, this paper proposed a novel robust and stable indoor localization method based on Wi-Fi RTT and PDR. This method a position-tracking adaptive EKF system with an outlier detection method in Wi-Fi RTT localization to decrease the measuring error. Then, a fusion algorithm is implemented to fuse Wi-Fi RTT and PDR. In addition, a fixed-interval smoothing method is introduced to correct the fusion localization error. The proposed method can achieve stable and robust indoor localization results in practical applications.

III. PROPOSED INDOOR LOCALIZATION SYSTEM

A. Overview

The overview of the proposed indoor localization system is shown in Fig. 1. The input of the system is the readings of Wi-Fi RTT, accelerometers, magnetometers, and gyroscopes receiver.

Firstly, a new outlier detection method is proposed. This method uses the sequence optimization error model to optimize the state estimation, and eliminates the detected outliers by checking the size of the residuals. Moreover, the position-tracking filter composed of a set of the same EKF is built based on the Wi-Fi RTT measurements and the corresponding standard deviation. Combined with the proposed outlier detection method, this bank of the EKF with different outlier detection thresholds runs in parallel

for the system EKF's statistical information. This scheme forms an adaptive optimal estimation based on RTT data. It calculates the weighted sum of estimates produced by each independent EKF, and then the system obtains the Euclidean distance between this value and the result of each independent EKF, and adjusts the weight according to the distance. Then, the system will dynamically automatically select the best filter and its estimated value. The detail of Wi-Fi RTT based position-tracking adaptive EKF is described in section III-B.

Secondly, a fusion-tracking federated filtering method based on observability is proposed to integrate Wi-Fi RTT and PDR results. In the initialization stage, the starting position of the PDR is determined by Wi-Fi RTT. During the localization process, the fusion results is used to calibrate the starting position of the PDR. The detail of the proposed fusion-tracking method is introduced in Section III-C.

Finally, a fixed-interval smoothing method is implemented to further reduce the localization error in this paper. Fixed-interval smoothing consists of two parts: backward filtering and weight-based fusion. During the time interval, this smoothing method uses backward filtering to process the localization results obtained from fusion-tracking FF. Then, the backward filtering results and fusing tracking results are weighted to obtain the smoothing localization results. Moreover, the smoothing results are used to eliminate the cumulative error of PDR. The detail of the smoothing method is introduced in section III-D.

B. Wi-Fi RTT-Based Position-Tracking Adaptive EKF

1) Ranging Principle of Wi-Fi RTT: Wi-Fi RTT is a new ranging protocol. The ranging principle of Wi-Fi RTT is shown in Fig. 2, Wi-Fi RTT signals are passed back and forth between devices which support the Wi-Fi RTT protocol. The distance is calculated based on the recorded time of the same signal between the base station and the smartphone [16]. The measurement equation is as follow:

$$T_{RTT} = \frac{1}{n} \sum_{k=1}^n ([t_4(k) - t_1(k)] - [t_3(k) - t_2(k)]), \quad (1)$$

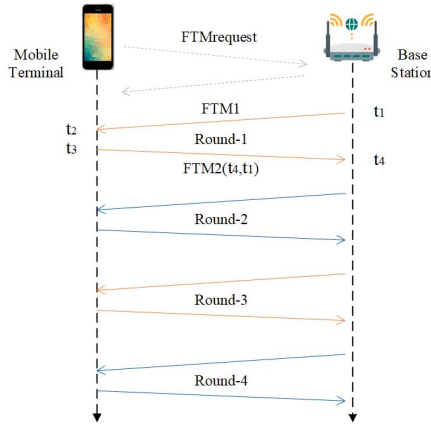


Fig. 2. The ranging principle of Wi-Fi RTT.

where T_{RTT} represents the time it takes to measure the distance from the smartphone to the device; $t_1(k)$ and $t_2(k)$ represent the timestamp of the signal on the smartphone; $t_3(k)$ and $t_4(k)$ represent the timestamp of the signal on the Wi-Fi RTT base station.

The distance from the smartphone to the base station is calculated by the following equation:

$$D_{RTT} = \frac{C}{2} \cdot T_{RTT}, \quad (2)$$

where D_{RTT} is Wi-Fi RTT measurement; C is the speed of light. At the same time, Wi-Fi RTT device will automatically calculate the corresponding measurement standard deviation.

2) Position-Tracking Adaptive EKF: In this section, the position-tracking adaptive EKF is implemented, includes EKF state model, EKF measurement model, time update, measurement update [29] and weighting scheme.

The EKF state model is:

$$\dot{x}(t) = F(t)x(t) + w(t), \quad (3)$$

where

$$F(t) = \begin{bmatrix} 1 & 0 & dt & 0 & dt^2/2 & 0 \\ 0 & 1 & 0 & dt & 0 & dt^2/2 \\ 0 & 0 & 1 & 0 & dt & 0 \\ 0 & 0 & 0 & 1 & 0 & dt \\ 0 & 0 & 0 & 0 & 1 & 0 \\ 0 & 0 & 0 & 0 & 0 & 1 \end{bmatrix}, \quad (4)$$

dt is the time interval; $w(t)$ is the process noise vector; $x(t)$ is the 6-dimensional error state vector, which is defined as

$$x(t) = [\mathbf{p}_{rtt} \ \mathbf{v}_{rtt} \ \mathbf{a}_{rtt}], \quad (5)$$

where \mathbf{p}_{rtt} , \mathbf{v}_{rtt} , \mathbf{a}_{rtt} are the position of the mobile station, velocity vectors and accelerometer vectors, respectively.

The EKF measurement model is:

$$z(t) = |\tilde{p}_{mobile} - \tilde{p}_{BS}| = H(t)x(t) + v(t), \quad (6)$$

where $z(t)$ is the distance from the mobile station to the base station; \tilde{p}_{mobile} and \tilde{p}_{BS} are the coordinates of the station and base station, respectively; $H(t)$ is the measurement matrix; $v(t)$ is the Wi-Fi RTT localization noise.

Algorithm 1 Adaptive EKF With Outlier Detection

```

input: State function F, initial position  $x_0$ , initial state matrix  $P_0^-$ , system noise Q, measurement noise  $R_t$  and measurement value  $z_t$ .
output: Position-tracking localization results  $\hat{x}_{k/k-1}$  and state matrix  $P_k$ .
1: Set weight  $\beta$  and several EKF with different detection threshold.
2: Calculate  $\hat{x}_{k/k-1}$ .
3: while A new set of measurements  $z_k$  is received do
4:   Reset weight  $\beta$ .
5:   Enter state optimization:
6:   Calculate innovation  $\sigma_k$ ;
7:   Calculate optimal value R, P, K.
8:   Calculate  $P_k$ .
9:   Calculate distance from  $x_t^-_{tmp}$  to any anchor as H in EKF.
10:  Calculate  $K_{k,\hat{x}_k}$ .
11:  Enter outlier detection:
12:  Calculate residuals:
13:  for each  $z_i$  in  $z_k$  do
14:    Judge whether  $v_k$  is greater than Experience threshold  $D_{thr}$ .
15:    Delete the  $z_k$  and  $R_k$  outside the threshold value.
16:  end for
17:  Return  $\hat{x}_{k/k-1}$ ,  $P_k$  for every EKF.
18:  Calculate results of system EKF.
19: end while
```

The EKF consists of time update and measurement update steps, which are given as [30]

Time update:

$$\hat{x}_{k/k-1} = \Phi_{k/k-1}\hat{x}_{k-1}, \quad (7)$$

$$P_{k/k-1} = \Phi_{k/k-1}\hat{P}_{k/k-1}\Phi_{k/k-1}^T, \quad (8)$$

Measurement update:

$$K_k = P_{k/k-1}H_k^T(H_kP_{k/k-1}H_k^T + R_k)^{-1}, \quad (9)$$

$$\hat{x}_k = \hat{x}_{k/k-1} + K_k(z_k - H_k\hat{x}_{k/k-1}), \quad (10)$$

$$P_k = (I - K_k H_k)P_{k/k-1}, \quad (11)$$

where “ \wedge ” denotes the state estimation; Subscript $k/k-1$ represents the recursive process from t_{k-1} to t_k ; P is the covariance matrix; K is the Kalman gain.

Adaptive process:

The process is to assign weights ($\beta_i, i = 1, 2, \dots, N$) equally at initialization time according to the total number (N) of EKF built. Each EKF in the bank of EKFs computes its own estimate, which is based on a different outlier detection threshold. The localization results in system EKF are calculated as follows:

$$\hat{x}_k = \sum_{i=1}^L \hat{x}_k^i \beta_i, \quad i = 1, 2, \dots, L, \quad (12)$$

where \hat{x}_k^i is estimate of each EKF, \hat{x}_k is estimate of system EKF.

The weight adjustment scheme uses the method in [31]. When the measurements evolve over time, the adaptive scheme will learn which EKF is correct, and when the other EKFs tend to zero, the weight coefficient of the adaptive scheme approaches one.

3) Outlier Detection: In this part, the outlier detection is implemented by using the innovation and residual error obtained in the position-tracking EKF, which forms a two-layer detection.

The first layer is optimization using the innovation sequence to estimate the measurement noise covariance to correct the state estimation [32]. The innovation sequence calculated within the EKF can be expressed as:

$$\sigma_k = z_k - H\hat{x}_{k/k-1} = He_k + \sigma_k, \quad (13)$$

where σ_k is a zero-mean Gaussian white noise sequence for an optimal filter; e_k is the error of the innovation sequence. However, for a suboptimal filter, the innovation sequence presents the following relationship.

Let

$$\Gamma_j = E\sigma_k\sigma_{k-j}^T, \quad (14)$$

Substituting equation (13) into equation (14), yields

$$\begin{aligned} \Gamma_j &= E(He_k + v_k)(He_{k-j} + v_{k-j})^T \\ &= HEe_k e_{k-j}^T + HEe_k\sigma_{k-j}^T \end{aligned} \quad (15)$$

When $j = 0$, equation (15) can be written as:

$$\Gamma_0 = HPH^T + R, \quad (16)$$

The expectation terms in (15) can be evaluated by writing the difference equation for e_k using (6)-(10). Assuming that the a priori gain K_0 is used for the suboptimal filter:

$$e_k = \Phi(I - K_0H)e_{i-1} - \Phi K_0\sigma_{i-1} + u_{i-1}, \quad (17)$$

By carrying equation (17) j steps back, we have

$$\begin{aligned} e_k &= [\Phi(I - K_0H)]^j e_{k-j} - \sum_{m=1}^j [\Phi(I - K_0H)]^{j-m} \\ &\quad \times \Phi K_0\sigma_{j-m} + \sum_{m=1}^j [\Phi(-K_0H)]^{j-m} u_{j-m}. \end{aligned} \quad (18)$$

Therefore,

$$E\sigma_k\sigma_{k-j}^T = [\Phi(I - K_0H)]^j P_1, \quad (19)$$

where $P_1 = E\sigma_k\sigma_k^T$. Replacing in (15) yield

$$\Gamma_j = H[\Phi(I - K_0H)]^{j-1}\Phi[P_1H^T - K_0\Gamma_0]. \quad (20)$$

For a filter,

$$K = PH^T[HPH^T + R]^{-1}, \quad (21)$$

Γ_j is not effectively used. When Q and R are accurately estimated as the measurements increases, both matrix P and gain K will be suboptimized. The optimal Q , R and K can

be obtained as follows: First, by transforming equation (20), we obtain:

$$\begin{aligned} P_1H^T &= (A^TA)^{-1}A^T \begin{bmatrix} \Gamma_1 + H\Phi K_0\Gamma_0 \\ \Gamma_2 + H\Phi K_0\Gamma_1 + H\Phi^2 K_0\Gamma_0 \\ \vdots \\ \Gamma_n + H\Phi K_0\Gamma_{N-1} + \dots + H\Phi^k K_0\Gamma_0 \end{bmatrix} \quad (22) \end{aligned}$$

where $k = 1, \dots, n$. Second, R can be calculated with Γ_0 and P_1H^T :

$$R = \Gamma_0 - H(P_1H^T). \quad (23)$$

Third, since covariance P and Kalman gain K are related, we can obtain from equations (8) and (12)

$$P = \Gamma(P - KHP)\Phi^T + Q. \quad (24)$$

Using (17), with simple derivation and replacement with (24), one obtains

$$\begin{aligned} P - P_1 &= \Phi[P - P_1 - KHP + K_0HP + P_1H^TK_0^T \\ &\quad - K_0(HP_1H^T + r)K_0^T]\Phi^T. \end{aligned} \quad (25)$$

Let $\delta P = P - P_1$. The optimal gain K can be written as

$$K = (P_1H^T + \delta PH^T)(C_0 + H\delta PH^T)^{-1}. \quad (26)$$

Substituting in (25),

$$\begin{aligned} \delta P &= \Phi[\delta P - (P_1H^T + \delta PH^T)(C_0 + H\delta PH^T)^{-1} \\ &\quad \times (HP_1 + H\delta P) + K_0HP_1 + P_1H^TK_0^T - K_0\Gamma_0K_0^T]\Phi^T. \end{aligned} \quad (27)$$

The derived $\hat{\Gamma}_j$ is

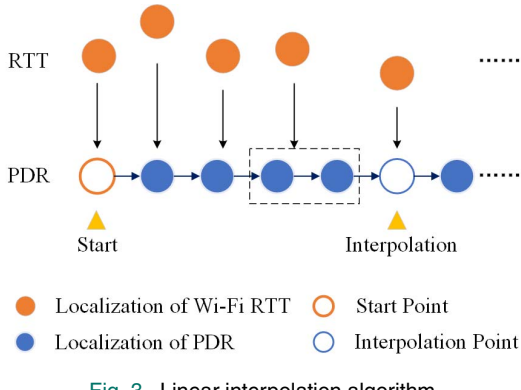
$$\hat{\Gamma}_j = \frac{1}{N} \sum_{i=j}^N \sigma_i\sigma_{i-j}^T. \quad (28)$$

where N is the number of data. In practical applications, the measurements z_k can be repeatedly used to optimize the state estimation. The innovation sequence will adaptively optimize the Gaussian noise matrix.

The second layer is the outlier detection. Since the residuals can reflect the measurement error, the outliers can be detected by comparing the residual size with an empirical threshold. The residual is calculated as follows:

$$v_k = z_k - H\hat{x}_{k/k-1}. \quad (29)$$

where $\hat{x}_{k/k-1}$ represents the results of Kalman filter. We compare the residuals v_k for each estimation value with the set threshold $D_{threshold}$. If $|v_k| > D_{threshold}$, this measurement is considered an outlier; otherwise, it is not an outlier. The measurements whose outliers are still too large will be eliminated, and the remaining measurements will be reused for the measurement update in the position-tracking EKF. Then, position-tracking EKF will re-estimate the state and proceed to the next cycle.



C. Fusion-Tracking FF Based on Wi-Fi RTT and PDR

1) **Principle of PDR:** PDR includes three steps: step detection, step length estimation and heading estimation [33], [34]. Step detection is realized by a peak detection algorithm based on the acceleration data. The existing models for step length estimation include linear models, nonlinear model and constant model [35]. The Weinberg model is used in this paper [36], and the step length estimation equation is as follows:

$$S_k = k \cdot \sqrt[4]{a_{max} - a_{min}}. \quad (30)$$

where k is the scale factor of the step length; a_{max} is the maximum acceleration in step k ; a_{min} is the minimum acceleration in step k . The three-axis gyroscope is used to implement the heading estimation [37].

2) **Fusion-Tracking Federated Filter Model:** In this section, a fusion method based on Wi-Fi RTT and PDR is introduced. The premise of multi-source sensor data fusion localization is that the same time stamp has corresponding localization data. The proposed method uses linear interpolation algorithm to solve the problem of inconsistent time stamps of two data. The detail of linear interpolation algorithm is shown in Fig. 3. PDR-based linear interpolation method is described as two steps: Firstly, two PDR localization results which is closest to the fusion timestamp are obtained. Secondly, the linear interpolation method is used to calculate the PDR for fusion. After interpolation, Wi-Fi RTT localization results and PDR are fused by fusion-tracking federated filter. This filter mainly includes four parts: information distribution and reset, information time update, measurement update and information fusion.

Information distribution and reset:

The system information, including the process information Q of the system, is distributed among each sub-filter. And use the fusion results X and P to reset each filter state.

$$Q_{W_{k-1}}^i = \beta_i^{-1} Q_{W_{k-1}}. \quad (31)$$

$$P_{k|k}^i = \beta_i^{-1} P_{k|k}^g, \quad \beta_i > 0 \text{ and } \sum_{i=1}^N \beta_i + \beta_m = 1. \quad (32)$$

$$\hat{x}_{k|k}^i = \hat{x}_{k|k}^g, \quad i = 1, 2, \dots, N, m. \quad (33)$$

where β is weight.

Information time update:

$$\hat{x}_{k|k-1}^i = F_{k-1} \hat{x}_{k-1}^i. \quad (34)$$

$$P_{k|k-1}^i = F_{k-1} P_{k|k-1}^i F_{k-1}^T + \Gamma_{k-1} Q_{W_{k-1}}^i \Gamma_{k-1}^T. \quad (35)$$

where $i = 1, 2, \dots, N, m$.

Measurement update:

There is no measurement update for the main filter, and the measurement update is only carried out in each local sub-filter.

$$(P_k^i)^{-1} = (P_{k|k-1}^i)^{-1} + (H_k^i)^T Q_{V_k^i}^{-1} (H_k^i). \quad (36)$$

$$(P_k^i)^{-1} \times \hat{x}_k^i = (P_{k|k-1}^i)^{-1} \hat{x}_{k|k-1}^i + (H_k^i)^T Q_{V_k^i}^{-1} z_k^i. \quad (37)$$

Information fusion:

$$P_k^g = [(P_1^1)^{-1} + \dots + (P_N^1)^{-1} + (P_m^1)^{-1}]^{-1}. \quad (38)$$

$$\hat{x}_k^g = P_k^g [(P_1^1)^{-1} \hat{x}_1^1 + \dots + (P_N^1)^{-1} \hat{x}_N^1 + (P_m^1)^{-1} \hat{x}_m^1]. \quad (39)$$

During the whole federated filter process, the weight of each sub-filter is given by the observability in the next section to improve the localization reliability.

The cumulative error of the PDR will increase throughout the process. Therefore, the fusion results will be used as the starting position and combined with the relative displacement to continue the recursion. This process is also the first correction of PDR.

3) **Observability:** This method introduces observability measure as the weighting factor of the federated filter. The observable formula can be expressed as

$$O(t_0, t_f) = \int_{t_0}^{t_f} \Phi^T(t, t_0) H^t H(t) \Phi(t, t_0) dt. \quad (40)$$

A new measurement vector is introduced:

$$Z_k^* = O_k X_k + v_k^*. \quad (41)$$

where

$$Z_k^* = \begin{bmatrix} Z_k \\ Z_{k+1} \\ \vdots \\ Z_{k+n-1} \end{bmatrix}, \quad v_k^* = \begin{bmatrix} v_k^* \\ v_{k+1}^* \\ \vdots \\ v_{k+n-1}^* \end{bmatrix}$$

$$= \begin{bmatrix} v_k \\ H_{k+1} \Gamma_k w_k + v_{k+1} \\ \vdots \\ H_{k+n-1} \Phi_{k+n-2} \dots \Phi_{k+1} \Gamma_k w_k + \dots + v_{k+n-1} \end{bmatrix}$$

Using the pseudo inverse of the observable matrix, the following relationship between the system error state and the measured values can be obtained.

$$X_k = O_k^+ Z_k^* - O_k^+ v_k^*. \quad (42)$$

where “+” represents the pseudo inverse of the matrix.

Construct the measurement vector $Y_k = O_k^+ Z_k^*$ and noise vector $\Lambda_k = O_k^+ v_k^*$ and express them as the following scalar forms.

$$Y_k^i = a_{1,k}^i Z_k + a_{2,k}^i Z_{k+1} + \dots + a_{n,k}^i Z_{k+n-1}. \quad (43)$$

$$\Lambda_k^i = a_{1,k}^i v_k^* + a_{2,k}^i v_{k+1}^* + \dots + a_{n,k}^i v_{k+n-1}^*. \quad (44)$$

Algorithm 2 Fixed-Interval Smoothing Algorithm

input: Fusing PDR and Wi-Fi RTT localization results $Z_f = [x_f^s, y_f^s, z_f^s], s = [N_f^t, N_f^{t+1}, \dots, N_f^{t+i}]$, T represents Time threshold, and timestamps $T_f^s, s = N_f^t, N_f^{t+1}, \dots, N_f^{t+i}$ from step 2.

output: Smoothing localization results $\hat{x}_{k/k-1}$ and state matrix P_k .

- 1: **if** $|N_f^{t+d} - N_f^t|$ quals to d(d=Time threshold) **then**
- 2: Initialize a new EKF filter
- 3: Set the last value of fusion-tracking EKF to the initial value
- 4: Start backward filtering.
- 5: **end if**
- 6: Calculate localization results based on weight factor.

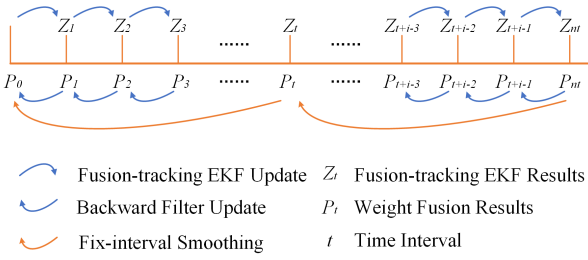


Fig. 4. Fixed-interval smoothing method.

where Y_k^i is the i -th component of the constructed measure vector Y_K , Λ_k^i is the i -th component of the constructed measure vector Λ_K . $a_{(j,k)}^i (j = 1, 2, \dots, k)$ is a member of the i -th row of O_K^+ .

Furthermore, the variance of measurement noise can be defined as

$$R_k^i = [(a_{1,k}^i)^2 + (a_{2,k}^i)^2 + \dots + (a_{n,k}^i)^2] R_k^0. \quad (45)$$

where R_k^0 is measuring the initial variance of the noise.

Therefore, the observability in a linear time-varying system can be expressed as

$$D_k^i = \frac{E_k[(X^i)^2]}{E_k[(Y^i)^2] \sum_{j=1}^n (a_{j,k}^i)}. \quad (46)$$

where

$$E_k[(X^i)^2] = \frac{1}{n} \sum_{j=k}^{k+n-1} (X_j^i)^2, E_k[(Y^i)^2] = \frac{1}{n} \sum_{j=k}^{k+n-1} (Y_j^i)^2.$$

For each state variable in the system, the observability is expressed as

$$d_k^i = \frac{e_k(X^i)}{e_k(Y^i) a_{\sum,k}^i}. \quad (47)$$

where $e_k(X^i) = \sqrt{E_k[(x^i)^2]}$, $e_k(Y^i) = \sqrt{E_k[(Y^i)^2]}$, $a_{\sum,k}^i = \sqrt{\sum_{j=1}^n (a_{j,k}^i)^2}$.

D. Fixed-Interval Smoothing Method

To enhance the robustness of the localization system, a fixed-interval smoothing method [38] is proposed.

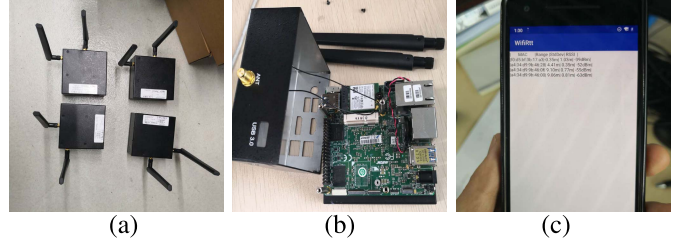


Fig. 5. Experimental device. (a) Wi-Fi RTT base station; (b) Mainboard of Wi-Fi RTT; (c) Smartphone (Pixel 2).

The smoothing process is shown in Fig. 4. Z_t represents fusion-tracking EKF result, which is updated in the direction of the blue arrow within the set time period P_t , and the results are shown as $(Z_1, Z_2, Z_3, \dots, Z_t)$. The backward filter will start to work when the same-interval fusion-tracking EKF is completed. The initial value of the backward filter is the end value of the fusion-tracking EKF. The backward filter results are shown as $(P_t, P_{t-1}, P_{t-2}, \dots, P_1)$. The final smoothing results are obtained by weighting the two filter results in the same interval. Since both forward and backward filtering results have deviations, the two filtering results are weighted, as the calculation method is shown in equation (48). The weight factor for fusing forward and backward filtering results is an empirical value. The end localization results of the forward filtering is used as the initial value of the backward filtering, this method is applied to each interval. Algorithm 3 provides the implementation process of the smoothing algorithm in detail.

$$P_{\text{weight}} = P_{\text{backward}} \cdot \delta_w + P_{\text{fusion}} \cdot \delta_w. \quad (48)$$

where δ_w is the empirical weight factor; P_{weight} is the smoothing results; P_{backward} and P_{fusion} are the backward filter results and fusion-tracking EKF results, respectively.

IV. EXPERIMENTAL RESULTS

A. Experimental Setup

Wi-Fi RTT base station with Intel®Cherry Trail x5-z8350 SoC as the kernel and frequency of 1.44 GHz was used in the experiments, as shown in Fig. 5(a) and Fig. 5(b). The Google Pixel 2 equipped a new chip with the IEEE 802.11-standardized Fine Time Measurement (FTM) was used as the mobile device, as shown in Fig. 5(c). The sampling frequencies of the inertial sensors and Wi-Fi RTT are 50 Hz and 1 Hz, respectively. The inertial sensors include accelerometer and gyroscope. The Wi-Fi RTT data includes the MAC address, distance measurements, standard deviation, and signal strength.

To evaluate the performance of the proposed indoor localization method, four experiments were conducted in different scenarios at Shenzhen University, including an office building, an indoor basketball stadium, and a school canteen. The layouts of the experiment areas are shown in Fig. 6. The two areas are rectangles with the sizes of $10 \times 10m^2$ and $6 \times 4m^2$, the other is an equicrural triangle, with the base of 6m, and height of 4.8 m. The last one is an experimental area in the actual pedestrian walkway of the office building.

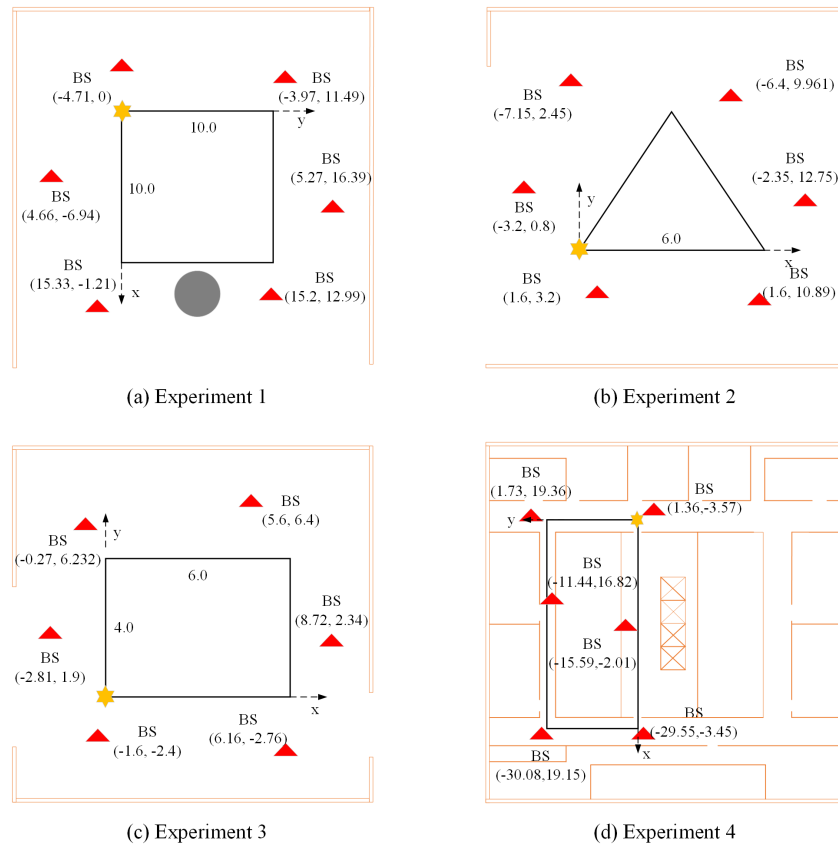


Fig. 6. Experiment area.

The experiment size is $32\text{ m} \times 21\text{ m}$. Six Wi-Fi RTT base stations were set up outside the test areas, as represented by the red triangles in Fig. 6. The yellow asterisk points represent the start points and end points, and the arrows represent the walking direction. The participants were asked to walk along the routes. The first three groups of experiments collected 10 laps of experimental data, and the last group of experiments collected 3 laps of experimental data. The TANGO RECORD software on the TANGO smartphone was used to collect the “ground truth” measurements.

All initial parameters of the EKF were set to empirical values, including initial state vector $x_{rtt} = [0\ 0\ 0\ 0\ 0\ 0]$, corresponding covariance matrix $P_{rtt} = [10\ 0\ 0\ 0\ 0\ 0; 0\ 10\ 0\ 0\ 0\ 0; 0\ 0\ 10\ 0\ 0\ 0; 0\ 0\ 0\ 10\ 0\ 0; 0\ 0\ 0\ 0\ 10\ 0; 0\ 0\ 0\ 0\ 0\ 10]$, and process noise matrix $Q_{rtt} = [1\ 1\ 0.1\ 0.1\ 0.01\ 0.01]$. The measurement noise matrix R_{rtt} was calculated using the standard deviation of Wi-Fi RTT. The same parameters were used in backward filter, except the initial values were set to the end values of the fusion-tracking EKF. The weight factor of fixed-interval smoothing method is set to 0.5 according to [37]. The time interval implemented in fixed-interval smoothing method is set to 60s.

B. Performance of Proposed Indoor Localization Method

Fig. 7, Fig. 8, Fig. 9, and Fig. 10 show the track of the four experiments respectively. The red circle represents the starting point of reference. The red dashed line represents the ground truth in each figure. The orange tracks in the four experiments

represent the walking tracks obtained using only the Wi-Fi RTT-based EKF algorithm. We can see that the track offset of the red track in Fig. 7 are much larger than that of the others. This is because there is a huge cylinder between the BS 3 and BS 4, which may seriously interfere with the Wi-Fi RTT signal, as shown in Fig. 6(a). The second and third experiments have better visibility, therefore their track offset is relatively small, as shown in Fig. 8 and Fig. 9. In Fig. 10, the experimental environment has the greatest influence on the signal of base stations, and the intervisibility between base stations is very poor. The localization results show that the performance of Wi-Fi RTT-based indoor localization is seriously affected by the visibility and multipath effect. The blue dotted tracks represent the Wi-Fi RTT localization results using the position-tracking adaptive EKF algorithm with outlier detection, as shown in Fig. 7(a), Fig. 8(a), Fig. 9(a), and Fig. 10(a). It is observed that the blue dotted tracks are closer to ground truth. The blue dashed tracks represent the fusion-tracking results based on Wi-Fi RTT and PDR. The solid blue tracks represent fixed-interval smoothing results. The three type of tracks have been greatly improved compared to the orange tracks and the estimated end positions are also closer to the actual ones in the four experiments.

Table I shows the average error results of our proposed method and the position-tracking EKF. As we can see in Table I that the average localization error obtained using classic EKF is 3.005m, 1.165m, 1.178m, and 4.664m, respectively. The average localization error of the blue dotted tracks

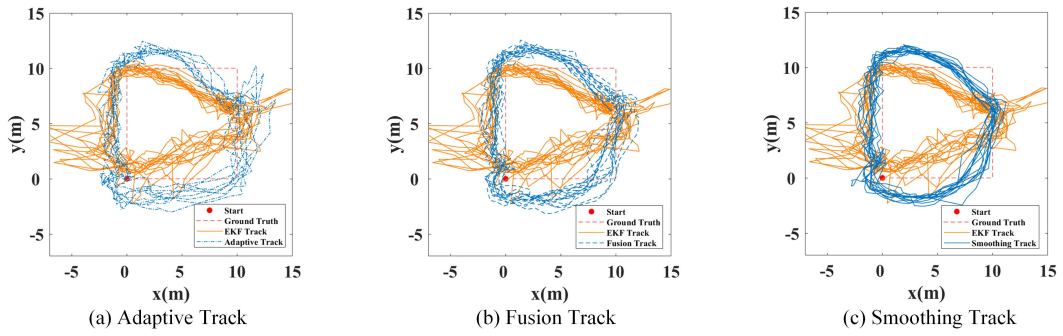


Fig. 7. First tracking result.

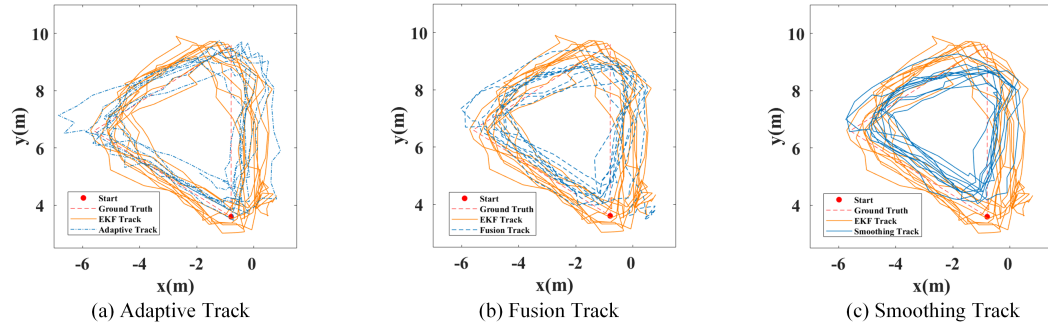


Fig. 8. Second tracking result.

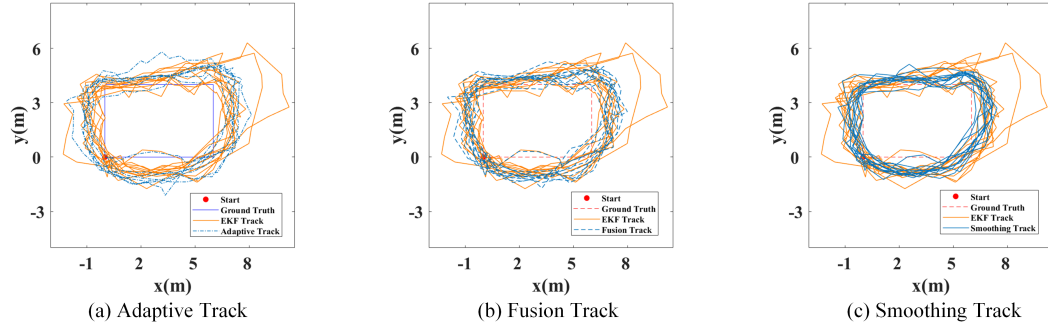


Fig. 9. Third tracking result.

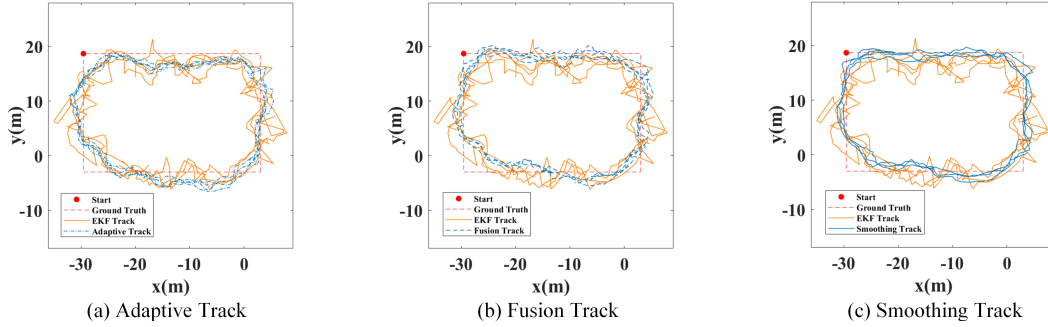


Fig. 10. Fourth tracking result.

obtained by the position-tracking adaptive EKF with outlier detection method decreases to 2.153m, 0.981m, 0.987m, and 2.841m, which increased by 28.4%, 12.8%, 16.2%, and 39.1%, respectively. After the fusion solution, the average accuracy of the localization results is reduced to 1.536m, 0.753m, 0.853m, and 1.925m, which improves 48.9%, 35.4%, 27.6%, and 58.7% respectively. The average localization error derived

from the smoothing method are further decreased to 1.324m, 0.719m, 0.738m, and 1.513m with 55.9%, 38.3%, 37.4%, and 67.6% reduction compared to the classic EKF results. The four sets of tracks have a significant improvement in localization accuracy.

Fig. 11 shows the Cumulative Distribution Function (CDF) of localization results based on the proposed method.

TABLE I
LOCALIZATION ERRORS OF PROPOSED METHOD

Method	Average Localization Error(m)			
	1st track	2nd track	3rd track	4th track
Classic EKF	3.005	1.165	1.178	4.664
Adaptive EKF	2.153	0.981	0.987	2.841
Fusion-tracking FF	1.536	0.753	0.853	1.925
Fixed-interval Smoothing	1.324	0.719	0.738	1.513

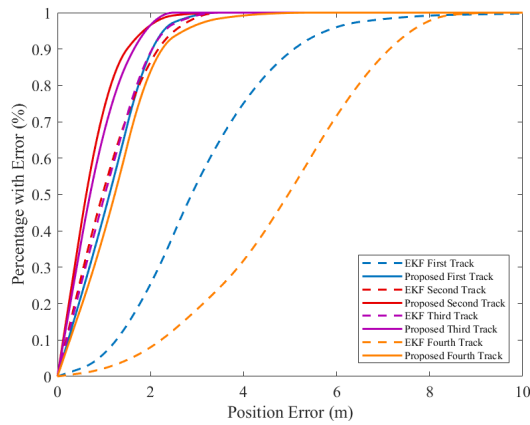


Fig. 11. CDF of position error.

TABLE II
LOCALIZATION ERRORS WITH DIFFERENT NUMBER OF BASE STATION

Number of anchors	3	4	5	6
1st track (m)	2.752	2.353	1.468	1.324
2nd track (m)	1.692	1.134	0.951	0.719
3rd track (m)	1.814	1.341	0.898	0.738
4rd track (m)	3.784	2.463	1.665	1.513

In track 1, it is observed that number of localization error within one meter reached 48.3%, and the number of localization errors within two meters reached 91.5%. In track 2, the number of localization error less than 1m increases from 53.6% to 85%. In track 3, the number of localization errors less than 1m increases from 40.2% to 83.4%. In track 4, the number of localization errors less than 1m reached 42.9%.

C. Influence of Number of Base Station

To evaluate the influence of the number of base stations on the proposed localization method, we conducted experiments with different numbers of base stations. The number of the base station is set from 3 to 6. The localization errors with different number of the base station are shown in Table II. It can be seen that when the number of base stations increases from 3 to 6, the localization error is decreasing gradually. For the first track, the localization error is 2.752m when the number of base station is 3, it decreases to 1.324m when the number of base station is set to 6. The other tracks have the same changing tendency with the first one. The errors of the next two tracks at 6 base stations are 0.719m and 0.738m

respectively. The errors of the fourth tracks at 6 base stations are 1.513m. Therefore, the localization error is the smallest when the number of base stations is 6.

V. CONCLUSION AND FUTURE WORK

This paper proposed a novel EKF-based data fusion method of Wi-Fi RTT and PDR for indoor localization using smartphone. Firstly, an adaptive filtering algorithm composed of EKF and outlier detection method is proposed to eliminate measurement errors. Secondly, we proposed a data fusion algorithm based on Wi-Fi RTT and PDR to further reduce errors and ensure localization stability. Finally, to improve robustness, a fixed-interval smoothing is implemented in our method. It uses a backward filter to perform a second noise reduction on the measurements, and then obtains the final localization results through a weighted fusion method. The algorithm proposed in this paper is constantly revising the PDR so that the cumulative error of the PDR will not affect the accuracy of the entire localization system. The performance of the proposed approach has been evaluated by experiments in four indoor environments. The results show that the proposed indoor localization method based on Wi-Fi RTT and PDR can realize stable, long-term and robust indoor localization.

ACKNOWLEDGMENT

Xu Liu, Weixing Xue, and Qingquan Li are with the College of Civil and Transportation Engineering, Shenzhen University, Shenzhen 518060, China, also with the Guangdong Key Laboratory of Urban Informatics, Shenzhen University, Shenzhen University, Shenzhen 518060, China, also with the Shenzhen Key Laboratory of Spatial Smart Sensing and Services, Shenzhen University, Shenzhen 518060, China, and also with the MNR Key Laboratory for Geo-Environmental Monitoring of Great Bay Area, Shenzhen University, Shenzhen 518060, China (e-mail: xuliuksy@126.com; wxxue@hotmail.com; liqq@szu.edu.cn).

Baoding Zhou and Jiasong Zhu are with the College of Civil and Transportation Engineering, Shenzhen University, Shenzhen 518060, China, and also with the Institute of Urban Smart Transportation and Safety Maintenance, Shenzhen University, Shenzhen 518060, China (e-mail: bdzhou@szu.edu.cn; zjsong@szu.edu.cn).

Panpan Huang is with the Hangzhou Innovation Institute, Beihang University, Hangzhou 310052, China (e-mail: hppbuaa@163.com).

Li Qiu is with the College of Mechatronics and Control Engineering, Shenzhen University, Shenzhen 518060, China (e-mail: qiu.li@szu.edu.cn).

REFERENCES

- [1] B. Zhou, Q. Li, Q. Mao, W. Tu, X. Zhang, and L. Chen, "ALIMC: Activity landmark-based indoor mapping via crowdsourcing," *IEEE Trans. Intell. Transp. Syst.*, vol. 16, no. 5, pp. 2774–2785, Oct. 2015.
- [2] W. Ma, Q. Li, B. Zhou, W. Xue, and Z. Huang, "Location and 3-D visual awareness-based dynamic texture updating for indoor 3-D model," *IEEE Internet Things J.*, vol. 7, no. 8, pp. 7612–7624, Aug. 2020.
- [3] L. Hou *et al.*, "Orientation-aided stochastic magnetic matching for indoor localization," *IEEE Sensors J.*, vol. 20, no. 2, pp. 1003–1010, Jan. 2020.
- [4] B. Zhou, Q. Li, Q. Mao, W. Tu, and X. Zhang, "Activity sequence-based indoor pedestrian localization using smartphones," *IEEE Trans. Human-Mach. Syst.*, vol. 45, no. 5, pp. 562–574, Oct. 2015.
- [5] B. Zhou, W. Tu, K. Mai, W. Xue, W. Ma, and Q. Li, "A novel access point placement method for WiFi fingerprinting considering existing APs," *IEEE Wireless Commun. Lett.*, vol. 9, no. 11, pp. 1799–1802, Nov. 2020.
- [6] A. Poulose, J. Kim, and D. S. Han, "A sensor fusion framework for indoor localization using smartphone sensors and Wi-Fi RSSI measurements," *Appl. Sci.*, vol. 9, no. 20, p. 4379, Oct. 2019.
- [7] Y. Zhuang, Y. Li, L. Qi, H. Lan, J. Yang, and N. El-Sheimy, "A two-filter integration of MEMS sensors and WiFi fingerprinting for indoor positioning," *IEEE Sensors J.*, vol. 16, no. 13, pp. 5125–5126, Jul. 2016.

- [8] Y. Zhuang, Z. Syed, Y. Li, and N. El-Sheimy, "Evaluation of two WiFi positioning systems based on autonomous crowdsourcing of handheld devices for indoor navigation," *IEEE Trans. Mobile Comput.*, vol. 15, no. 8, pp. 1982–1995, Aug. 2016.
- [9] X. Li, K. Pahlavan, M. Latva-aho, and M. Ylanttila, "Comparison of indoor geolocation methods in DSSS and OFDM wireless LAN systems," in *Proc. Veh. Technol. Conf. Fall IEEE VTS Fall VTC. 52nd Veh. Technol. Conf.*, Sep. 2002, pp. 3015–3020.
- [10] D. D. McCrady, L. Doyle, H. Forstrom, T. Dempsey, and M. Martorana, "Mobile ranging using low-accuracy clocks," *IEEE Trans. Microw. Theory Techn.*, vol. 48, no. 6, pp. 951–958, Jun. 2000.
- [11] A. Gänther and C. Hoene, "Measuring round trip times to determine the distance between WLAN nodes," in *Proc. Int. Conf. Res. Netw.* Cham, Switzerland: Springer, 2005, pp. 768–779.
- [12] Y. Zhuang, Z. Syed, J. Georgy, and N. El-Sheimy, "Autonomous smartphone-based WiFi positioning system by using access points localization and crowdsourcing," *Pervas. Mobile Comput.*, vol. 18, pp. 118–136, Apr. 2015.
- [13] Y. Cheng, X. Wang, M. Morelande, and B. Moran, "Information geometry of target tracking sensor networks," *Inf. Fusion*, vol. 14, no. 3, p. 311–326, 2013.
- [14] P. Bahl and V. N. Padmanabhan, "RADAR: An in-building RF-based user location and tracking system," in *Proc. IEEE INFOCOM Conf. Comput. Commun. 19th Annu. Joint Conf. IEEE Comput. Commun. Societies*, Mar. 2000, pp. 775–784.
- [15] Y. Amizur, U. Schatzberg, and L. Banin, "Next generation indoor positioning system based on WiFi time of flight," in *Proc. 26th Int. Tech. Meeting Satell. Division Inst. Navigat. (ION GNSS+)*, Mar. 2013, pp. 775–784.
- [16] M. Ibrahim *et al.*, "Verification: Accuracy evaluation of WiFi fine time measurements on an open platform," in *Proc. 24th Annu. Int. Conf. Mobile Comput. Netw.*, Oct. 2018, pp. 417–427.
- [17] A. Poulose, O. Steven Eyobu, and D. Seog Han, "An indoor position-estimation algorithm using smartphone IMU sensor data," *IEEE Access*, vol. 7, pp. 11165–11177, 2019.
- [18] W. Kang and Y. Han, "SmartPDR: Smartphone-based pedestrian dead reckoning for indoor localization," *IEEE Sensors J.*, vol. 15, no. 5, pp. 2906–2916, May 2015.
- [19] Y. Li, Y. Zhuang, P. Zhang, H. Lan, X. Niu, and N. El-Sheimy, "An improved inertial/WiFi/magnetic fusion structure for indoor navigation," *Inf. Fusion*, vol. 34, pp. 101–119, Mar. 2017.
- [20] C. Ma, B. Wu, S. Poslad, and D. R. Selviah, "Wi-Fi RTT ranging performance characterization and positioning system design," *IEEE Trans. Mobile Comput.*, early access, Jul. 28, 2020, doi: 10.1109/TMC.2020.3012563.
- [21] G. Guo, R. Chen, F. Ye, X. Peng, Z. Liu, and Y. Pan, "Indoor smartphone localization: A hybrid WiFi RTT-RSS ranging approach," *IEEE Access*, vol. 7, pp. 176767–176781, 2019.
- [22] S. Yan, H. Luo, F. Zhao, W. Shao, Z. Li, and A. Crivello, "Wi-Fi RTT based indoor positioning with dynamic weighted multidimensional scaling," in *Proc. Int. Conf. Indoor Positioning Indoor Navigat. (IPIN)*, Sep. 2019, pp. 1–8.
- [23] A. Poulose, B. Senouci, and D. S. Han, "Performance analysis of sensor fusion techniques for heading estimation using smartphone sensors," *IEEE Sensors J.*, vol. 19, no. 24, pp. 12369–12380, Dec. 2019.
- [24] X. Tao, X. Zhang, F. Zhu, F. Wang, and W. Teng, "Precise displacement estimation from time-differenced carrier phase to improve PDR performance," *IEEE Sensors J.*, vol. 18, no. 20, pp. 8238–8246, Oct. 2018.
- [25] C. Huang, Z. Liao, and L. Zhao, "Synergism of INS and PDR in self-contained pedestrian tracking with a miniature sensor module," *IEEE Sensors J.*, vol. 10, no. 8, pp. 1349–1359, Aug. 2010.
- [26] Y. Yu, R. Chen, L. Chen, G. Guo, F. Ye, and Z. Liu, "A robust dead reckoning algorithm based on Wi-Fi FTM and multiple sensors," *Remote Sens.*, vol. 11, no. 5, p. 504, Mar. 2019.
- [27] M. Sun, Y. Wang, S. Xu, H. Qi, and X. Hu, "Indoor positioning tightly coupled Wi-Fi FTM ranging and PDR based on the extended Kalman filter for smartphones," *IEEE Access*, vol. 8, pp. 49671–49684, 2020.
- [28] S. Xu, R. Chen, Y. Yu, G. Guo, and L. Huang, "Locating smartphones indoors using built-in sensors and Wi-Fi ranging with an enhanced particle filter," *IEEE Access*, vol. 7, pp. 95140–95153, 2019.
- [29] Y. Liu, S. Li, Q. Fu, Z. Liu, and Q. Zhou, "Analysis of Kalman filter innovation-based GNSS spoofing detection method for INS/GNSS integrated navigation system," *IEEE Sensors J.*, vol. 19, no. 13, pp. 5167–5178, Jul. 2019.
- [30] A. F. Garcia-Fernandez, L. Svensson, M. R. Morelande, and S. Sarkka, "Posterior linearization filter: Principles and implementation using sigma points," *IEEE Trans. Signal Process.*, vol. 63, no. 20, pp. 5561–5573, Oct. 2015.
- [31] D. Magill, "Optimal adaptive estimation of sampled stochastic processes," *IEEE Trans. Autom. Control*, vol. AC-10, no. 4, pp. 434–439, Oct. 1965.
- [32] R. K. Mehra, "Approaches to adaptive filtering," *IEEE Trans. Autom. Control*, vol. AC-17, no. 5, pp. 693–698, Oct. 1972.
- [33] V. Renaudin, M. Susi, and G. Lachapelle, "Step length estimation using handheld inertial sensors," *Sensors*, vol. 12, no. 7, pp. 8507–8525, Jun. 2012.
- [34] R. Harle, "A survey of indoor inertial positioning systems for pedestrians," *IEEE Commun. Surveys Tuts.*, vol. 15, no. 3, pp. 1281–1293, 3rd Quart., 2013.
- [35] P. Davidson and R. Piche, "A survey of selected indoor positioning methods for smartphones," *IEEE Commun. Surveys Tuts.*, vol. 19, no. 2, pp. 1347–1370, 2nd Quart., 2017.
- [36] H. Weinberg, "Using the ADXL202 in pedometer and personal navigation applications," Analog Devices Appl. Notes AN-602, 2002, p. 1–6, vol. 2.
- [37] R. Chen, L. Pei, and Y. Chen, "A smart phone based PDR solution for indoor navigation," in *Proc. Int. Tech. Meeting Satell. Division Inst. Navigat.*, vol. 10, no. 1, 2011, pp. 1404–1408.
- [38] A. Gelb, *Applied Optimal Estimation*. Cambridge, MA, USA: MIT Press, 1974.



Xu Liu received the B.E. degree in geomatics engineering from the Chengdu University of Technology, China, in 2016, and the M.E. degree in geodesy and geomatics engineering from the Kunming University of Science and Technology, China, in 2019. He is currently a Research Assistant with Shenzhen University. His research interests include indoor localization, computer vision, and mapping.



Baoding Zhou received the Ph.D. degree in photogrammetry and remote sensing from Wuhan University, Wuhan, China, in 2015.

He is currently an Assistant Professor with the College of Civil and Transportation Engineering, Shenzhen University, Shenzhen, China. His research interests include indoor localization and mapping, mobile computing, and intelligent transportation.



Panpan Huang received the B.E. degree in control technology and instrument from the Inner Mongolia University of Technology, Hohhot, China, in 2012, the M.E. degree in navigation, guidance and control from Beihang University, Beijing, China, in 2015, and the Ph.D. degree in surveying and spatial information systems from the University of New South Wales, Sydney, NSW, Australia, in 2019. She is currently a Postdoctoral Research Fellow with the Hangzhou Innovation Institute, Beihang University, Hangzhou, China. Her research interests include nonlinear filtering methods, high precision multi-GNSS/PPP positioning, and bio-inspired navigation systems.



Weixing Xue was born in Luyi, China, in 1990. He received the Ph.D. degree from the School of Geodesy and Geomatics, Wuhan University, Wuhan, China, in 2019. He is currently a Postdoctoral Researcher with the Shenzhen Key Laboratory of Spatial Smart Sensing and Service, College of Civil Engineering, Shenzhen University, Shenzhen, China. His research interests include seamless positioning and navigation, multisensor information fusion and data processing theory, and precision engineering measurement.



Qingquan Li received the Ph.D. degree in geographic information system and photogrammetry from the Wuhan Technical University of Surveying and Mapping, Wuhan, China, in 1998. He is currently a Professor with Shenzhen University, Shenzhen, China, and Wuhan University, Wuhan. His research interests include 3-D and dynamic data modeling in GIS, location-based service, surveying engineering, integration of GIS, global positioning system and remote sensing, intelligent transportation systems, and road surface checking.



Jiasong Zhu received the B.E. degree from the Huazhong University of Science and Technology, Wuhan, China, in 1997, the M.E. degree from Wuhan University, Wuhan, in 2003, and the Ph.D. degree from The University of Hong Kong, Hong Kong, in 2008.

He is currently a Professor with the College of Civil Engineering, Shenzhen University, Shenzhen, China. His research interests include multisensor integration and data fusion, high-resolution image processing, and GIS applications in urban planning and transportation.



Li Qiu (Member, IEEE) received the M.E. and Ph.D. degrees in control theory and control engineering from the South China University of Technology, Guangzhou, China, in 2006 and 2011, respectively. From August 2016 to August 2017, she was a Visiting Scholar with the Department of Mechanical Engineering, University of Victoria, Victoria, BC, Canada. She is currently working with the College of Mechatronics and Control Engineering, Shenzhen University. Her current research interests include networked control systems, Markovian jump linear systems and robust control, and control of switched reluctance motors and generators.